CASE RECORDS of the MASSACHUSETTS GENERAL HOSPITAL

Case 3-2025: A 54-Year-Old Man with Exertional Dyspnea and Chest Pain

Clyde W. Yancy, M.D., J. Sawalla Guseh II, M.D., Brian G. Ghoshhajra, M.D., Rodney H. Falk, M.D., Andrew J. Yee, M.D., and Bailey M. Hutchison, M.D.

PRESENTATION OF CASE

Dr. J. Sawalla Guseh II: A 54-year-old male athlete was evaluated in the cardiovascular performance program clinic of this hospital because of progressive exertional dyspnea and chest pain.

The patient had been in his usual state of health, including engaging in regular vigorous exercise, until 17 months before the current presentation, when intermittent nonradiating chest pressure and dyspnea on exertion developed. He felt unable to "get a full breath" during high-intensity aerobic exercise.

The only other history of chest discomfort was an episode of dull chest pain on the left side lasting 2 days, which had occurred after airline travel 5 years before the current presentation. On evaluation at that time, the blood level of troponin was normal, and an electrocardiogram showed sinus bradycardia.

Dr. Brian G. Ghoshhajra: Five years before the current presentation, coronary computed tomographic angiography (CTA) was performed according to an accelerated diagnostic protocol for chest pain. The patient had a Coronary Artery Disease Reporting and Data System (CAD-RADS) score of 0 (range, 0 to 5, with higher scores indicating more atherosclerotic plaque or severe stenosis) and a coronary-artery calcium score of 0, indicating no calcifications. He had no luminal narrowing or noncalcified plaque (Fig. 1A). The heart chambers were morphologically normal (i.e., normal size and normal wall thickness at end diastole), and the imaging findings were consistent with preserved resting systolic function of the left ventricle (Fig. 1B).

Dr. Guseh: One month after the onset of intermittent chest pressure and dyspnea on exertion, and 16 months before the current presentation, the patient was evaluated by his primary care physician. On examination, there was a grade 2/6 midsystolic murmur that had not been previously identified. Electrocardiography was performed and reportedly showed sinus rhythm, new rightward axis, reduced R-wave progression, and new inferolateral T-wave inversions, as compared with the electrocardiogram obtained 5 years before the current presentation. Findings on chest radiography were reportedly normal, as were results of laboratory tests,

From the Department of Medicine, Northwestern Memorial Hospital, Chicago (C.W.Y.); and the Departments of Medicine (J.S.G., A.J.Y.), Radiology (B.G.G.), and Pathology (B.M.H.), Massachusetts General Hospital, the Departments of Medicine (J.S.G., R.H.F., A.J.Y.), Radiology (B.G.G.), and Pathology (B.M.H.), Harvard Medical School, and the Department of Medicine, Brigham and Women's Hospital (R.H.F.) — all in Boston.

N Engl J Med 2025;392:383-94.
DOI: 10.1056/NEJMcpc2300900

CME

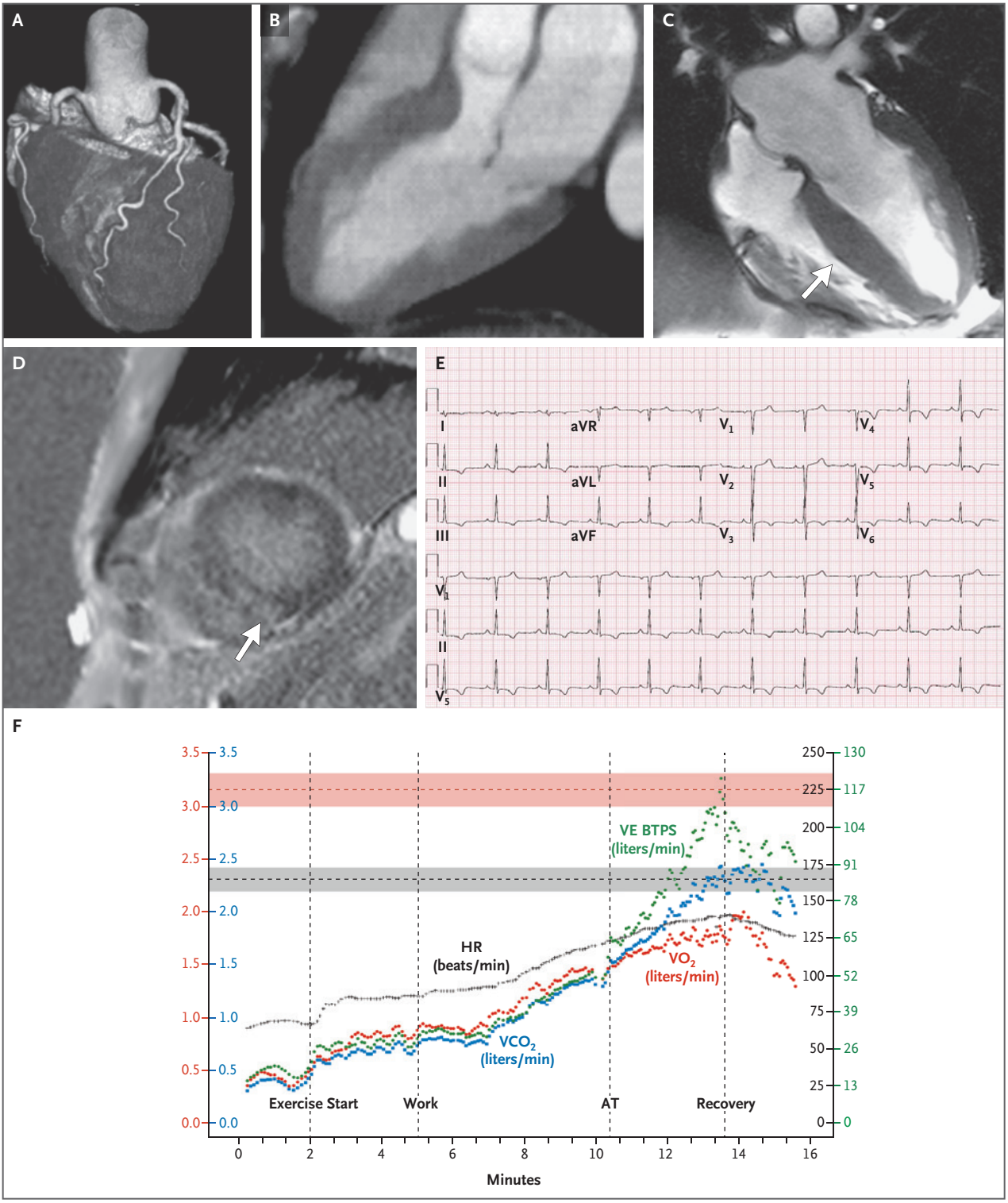

including a complete blood count, measures of kidney function, and blood levels of electrolytes, aspartate aminotransferase, alanine aminotransferase, albumin, total protein, iron, D-dimer, and thyrotropin. Treatment with aspirin was started, and additional cardiac testing was planned.

Figure 1 (facing page). Initial Diagnostic Tests.

An image from coronary computed tomographic angiography (CTA) was obtained 5 years before the current presentation (Panel A). No evidence of coronary stenosis or calcified or noncalcified plaque is present. The origins of the right and left arteries are normal. A shallow, proximal left anterior descending coronary artery bridge is visible. Cine images inclusive of end systole and end diastole were obtained (Panel B). Wall motion is normal (not shown), as are the end-diastolic wall thicknesses. A cardiac MRI image was obtained 14 months before the current presentation, with the use of cine-balanced steady-state free precession imaging, at end diastole in the four-chamber long-axis view (Panel C). Concentric left ventricular wall thickening of up to 18 mm is present (arrow), and there is a lack of tapering of the wall thickness from the base to the apex. A phase-sensitive inversion-recovery prepared late gadolinium enhancement image optimized for nulling of normal enhancement in the short axis of the mid-left ventricle (Panel D) shows low-level nonischemic, nonterritorial abnormal late gadolinium enhancement present in the midwall of the apical interventricular septum (arrow), with a total ventricular enhancement quantitated at 3% of the myocardial mass. An electrocardiogram obtained at the current presentation (Panel E) shows sinus rhythm, rightward axis, diffuse T-wave inversions, and diminished R-wave amplitudes in a septal distribution (leads V_1 and V_2) and high lateral distribution (leads I and aVL). Cardiopulmonary exercise test results (Panel F) are shown for oxygen consumption (VO_2, red), carbon dioxide production (VCO_2, blue), heart rate (HR, black), and minute ventilation (VE, green) as measured over time. Horizontal dashed lines denote 100% predicted heart rate (black) and oxygen consumption (red) based on healthy age- and sex-matched controls. The patient reached normal peak work output (213 watts, 100% of the predicted value) but had severely abnormal peak oxygen consumption (19.7 ml per kilogram per minute, 59% of the predicted value). AT denotes anaerobic threshold, and BTPS body temperature and pressure, saturated.

Ten days later, the patient underwent stress echocardiography. An electrocardiogram obtained when the patient was at rest reportedly showed T-wave inversions, and an echocardiogram reportedly showed a hyperdynamic left ventricle with mild mitral regurgitation. After 11 minutes of bicycle exercise, mild chest pressure and dyspnea developed, along with horizontal and downsloping ST depressions (2 mm) in the inferolateral leads, but no inducible left ventricular wall-motion abnormalities were detected.

Six weeks later, and 14 months before the current presentation, the patient was evaluated in the cardiology clinic of this hospital. He reported ongoing intermittent chest pressure and dyspnea on exertion during rigorous exercise. The physical examination was reportedly normal. Electrocardiography showed T-wave inversions that were more pronounced than those seen on previous imaging studies and a new Q wave in lead aVL. Transthoracic echocardiography showed a hyperdynamic left ventricle with symmetric wall thickening (17 mm), systolic intracavitary left ventricular obliteration without an outflow-tract or midcavity gradient, biatrial and inferior vena cava dilatation, right ventricular wall thickening, and mitral valve thickening. Additional imaging studies were performed.

Dr. Ghoshhajra: Cardiac magnetic resonance imaging (MRI), performed according to the diagnostic protocol for workup of suspected hypertrophic cardiomyopathy, confirmed concentric left ventricular wall thickening of up to 18 mm and a lack of tapering of the left ventricular wall thickness from the base to the apex (Fig. 1C). No evidence of myocardial edema was present; however, focal late gadolinium enhancement (defined as 6 SD above the reference signal intensity) affecting 3% of the left ventricular myocardium was present in the midwall apical interventricular septum (Fig. 1D). The anterior mitral leaflet appeared to be mildly elongated. These findings were suggestive but not diagnostic of hypertrophic cardiomyopathy.

Dr. Guseh: Holter monitoring showed occasional ectopic beats, with one 3-beat ventricular run and short supraventricular runs. A genetic testing panel that assessed for 56 genes associated with hypertrophic cardiomyopathy, including the genes encoding myosin, titin, lamin, transthyretin, and the γ2 subunit of AMP-activated protein kinase, was negative. The patient's adult children underwent echocardiography for screening purposes and were negative for thickened ventricular walls.

During the next year, the patient's symptoms persisted. A repeat stress echocardiogram showed mild mitral regurgitation at peak stress, with a peak left ventricular outflow-tract gradient of 12 mm Hg; blood pressure increased appropriately with exercise. He was referred to the cardiovascular performance program clinic of this hospital for cardiopulmonary exercise testing, exercise guidance, and an exercise prescription.

In the cardiovascular performance program clinic, the patient reported lifelong athletic pursuits,

including playing several sports in college and maintaining a vigorous exercise regimen of cycling, hockey, and rowing after college; he began competing in triathlons during his fourth decade of life. He described an insidious but progressive decline in exercise tolerance during the 17 months before the current presentation, which was accompanied by an increasing difficulty in recovery after exercise. He reported upper abdominal discomfort and bloating that occurred when he walked his dog after eating and a 2-week history of hoarseness. In addition, he reported no syncope, lightheadedness, palpitations, diaphoresis, or flushing. He had had no edema, orthopnea, paroxysmal nocturnal dyspnea, weight change, bruising or bleeding, or neurologic symptoms. He had not been vaccinated against severe acute respiratory syndrome coronavirus 2.

The patient's medical history included arthritis, surgeries to repair tears in both rotator cuffs, meniscectomies in both knees, and colonic polyps. Medications included aspirin; he had no known adverse reactions to medications. The patient worked as an executive, and he lived in suburban New England with his family. He drank alcohol socially and had used intranasal cocaine in the remote past; he had never used tobacco. His family history included premature coronary artery disease and heart failure in his father; hypertension, atrial fibrillation, and heart failure in his mother; and dyslipidemia in multiple relatives.

On examination, the heart rate was 81 beats per minute and the blood pressure 116/70 mm Hg. The jugular venous pressure was 13 cm of water, and Kussmaul's sign was present. Small angiomas (<4 mm) were noted on the truncal skin. The remainder of the examination was normal.

An electrocardiogram obtained when the patient was at rest showed sinus rhythm, rightward axis, T-wave inversions, and decreased QRS amplitudes, as compared with the electrocardiogram obtained 5 years before the current presentation (Fig. 1E). Cardiopulmonary exercise testing (Fig. 1F) revealed reduced maximal oxygen consumption at 19.7 ml per kilogram of body weight per minute (59% of the predicted value, as compared with age- and sex-matched nonathletic controls), a ventilatory threshold at 83% of peak oxygen consumption, and impaired oxygen pulse augmentation, which is a surrogate for stroke volume augmentation. Since the patient had normal spirometry and oxygenation, these findings suggested severe exercise impairment due to cardiovascular limitation.

The blood levels of albumin, globulin, total protein, and thyrotropin were normal. Other laboratory test results are shown in Table 1.

Furosemide and spironolactone were prescribed, and diagnostic tests were performed.

DIFFERENTIAL DIAGNOSIS

Dr. Clyde W. Yancy: In this 54-year-old high-performing male athlete, an insidious decline in functional capacity and progressively worsening exertional dyspnea developed over a period of 17 months. Coronary CTA performed 5 years before the current presentation had ruled out ischemic heart disease. Echocardiography performed 3 months after the onset of dyspnea on exertion revealed left ventricular wall thickening, which had not been present on the previous coronary CTA. Thickened ventricular walls can develop in athletes who engage in rigorous endurance and strength training. However, this condition is usually associated with both eccentric hypertrophy and ventricular dilatation, which were not observed in this patient. In addition, left ventricular wall thickness in athletes typically measures 13 to 15 mm; the 17-mm left ventricular wall thickness seen on this patient's echocardiogram makes athletic cardiac hypertrophy an unlikely diagnosis, and evaluation for other causes of left ventricular wall thickening was indicated.[1]

HYPERTROPHIC CARDIOMYOPATHY

In the absence of a history of hypertension, left ventricular wall thickening is indicative of cardiomyopathy.[1,2] Initially, a diagnosis of hypertrophic cardiomyopathy was considered in this patient. The biventricular thickening, mild anterior mitral leaflet elongation, and late gadolinium enhancement observed on this patient's cardiac MRI is consistent with hypertrophic cardiomyopathy. Although he did not have features of obstruction on stress echocardiography, the absence of this finding does not rule out hypertrophic cardiomyopathy. None of his adult children had features of hypertrophic cardiomyopathy on echocardiography; however, an absence of findings in the children does not change the likelihood of hypertrophic cardiomyopathy in the

Table 1. Laboratory Data.*

Variable	Reference Range, Adults†	On Initial Consultation, Cardiac Performance Program Clinic
Sodium (mmol/liter)	136–145	140
Potassium (mmol/liter)	3.6–5.1	4.5
Chloride (mmol/liter)	98–107	103
Carbon dioxide (mmol/liter)	22–32	28
Urea nitrogen (mg/dl)	6–20	25
Creatinine (mg/dl)	0.60–1.30	1.10
Calcium (mg/dl)	8.9–10.3	10.6
Alanine aminotransferase (U/liter)	10–55	55
Aspartate aminotransferase (U/liter)	10–40	53
Alkaline phosphatase (U/liter)	45–115	84
Total bilirubin (mg/dl)	0.0–1.0	0.7
High-sensitivity troponin T (ng/liter)	0–9	91
N-terminal pro–B-type natriuretic peptide (pg/ml)	<900	2099

* To convert the values for urea nitrogen to millimoles per liter, multiply by 0.357. To convert the values for creatinine to micromoles per liter, multiply by 88.4. To convert the values for calcium to millimoles per liter, multiply by 0.250. To convert the values for bilirubin to micromoles per liter, multiply by 17.1.

† Reference values are affected by many variables, including the patient population and the laboratory methods used. The ranges used at Massachusetts General Hospital are for adults who are not pregnant and do not have medical conditions that could affect the results. They may therefore not be appropriate for all patients.

patient, since their father's genotype might not have been inherited by the children, or features of the disease might not yet have manifested. Of note, recent commercial genetic testing in the patient did not detect any of the most common genetic causes of hypertrophic cardiomyopathy. Although a genetically acquired hypertrophic cardiomyopathy cannot be definitively ruled out, the time course of this patient's progressive symptoms, over 17 months, would be unexpected. An alternative explanation for the exertional dyspnea should be considered.

RESTRICTIVE CARDIOMYOPATHY

Several features of this patient's physical examination and cardiac testing are suggestive of restrictive physiology. Kussmaul's sign was identified on examination in the cardiac performance program clinic. Normally, decreased intrathoracic pressure during inspiration causes an increase in venous return to the heart with a corresponding decrease in jugular venous pressure. Kussmaul's sign is either the absence of a decrease or a paradoxical increase in jugular venous pressure during inspiration attributed to inability of the right ventricle to accommodate an increase in venous return. Kussmaul's sign is observed in patients with diseases that lead to impaired right ventricular filling, including right ventricular infarction, constrictive pericarditis, and restrictive cardiomyopathies.

Electrocardiography showed decreasing QRS voltage, as compared with findings seen 5 years before the current presentation, despite the left ventricular wall thickening observed on echocardiography. These findings are consistent with left ventricular wall thickening due to an infiltrative myocardial disease, several of which cause restrictive cardiomyopathy. Echocardiography showed not only thickened ventricular walls but also biatrial enlargement with normal ventricular chamber sizes, a pattern consistent with restrictive physiology. This pattern was further corroborated by cardiopulmonary exercise testing, which showed findings consistent with reduced stroke volume augmentation in response to exercise despite intact ventricular function. In this patient, restrictive physiology due to a disorder causing restrictive cardiomyopathy is the most likely diagnosis.

Noninfiltrative diseases associated with restrictive cardiomyopathy include systemic sclerosis,

diabetic cardiomyopathy, hypereosinophilic syndrome, endocardial fibroelastosis, and idiopathic disorders (including those caused by mutations in genes encoding desmin and sarcomeric proteins).[2,3] Noninfiltrative diseases are not likely causes of cardiomyopathy in this patient on the basis of the clinical history, presenting symptoms, and time course of the illness.

Hydroxychloroquine permeates myocytes and induces an acquired lysosomal storage disease that can lead to cardiomyopathy, although this usually occurs after several years of hydroxychloroquine use.[4] Given that this patient's symptoms developed during the coronavirus disease 2019 (Covid-19) pandemic, I would ask the patient about undisclosed use of hydroxychloroquine.

Storage diseases associated with restrictive cardiomyopathy include Fabry's disease, Gaucher's disease, and glycogen storage diseases.[2,3] Although this patient had angiomas on the skin, he had no other findings that would be consistent with Fabry's disease or any other of the storage diseases.

INFILTRATIVE DISEASES CAUSING CARDIOMYOPATHY

Sarcoidosis, an infiltrative disease characterized by noncaseating granulomas, is associated with restrictive cardiomyopathy.[3] Lymphadenopathy is a common manifestation of the disease. Mediastinal lymphadenopathy can lead to compression of the left recurrent laryngeal nerve, which results in vocal cord paralysis and hoarseness.[5] Sarcoidosis can also involve the vocal cords directly. Given that a history of hoarseness was reported in this patient's review of symptoms, sarcoidosis remains a possible diagnosis in this case.

Amyloidosis can be complicated by restrictive cardiomyopathy through the deposition of abnormal proteins in the myocardium. This patient's history of ligamentous disease (i.e., tears in both rotator cuffs) may provide an important clue. The original description of ligamentous disorders associated with amyloidosis included not only carpal tunnel syndrome and lumbar canal stenosis but also rotator-cuff tears.[6]

I suspect that this patient has a progressive symptomatic restrictive cardiomyopathy, most likely due to cardiac amyloidosis. To establish a diagnosis of amyloidosis, I would obtain levels of serum free light chains and a fat-pad biopsy specimen for Congo red staining and typing of protein.

CLINICAL IMPRESSION

Dr. Guseh: On evaluation of this patient with suspected hypertrophic cardiomyopathy, we were struck by his rapid decline in exercise capacity and the objectively reduced peak oxygen consumption on cardiopulmonary exercise testing, in contrast with his previously high level of aerobic fitness. The tempo of the decline and the finding of Kussmaul's sign led us to consider restrictive cardiomyopathies and disorders that mimic hypertrophic cardiomyopathy. Since some features of this patient's presentation were suggestive of amyloidosis, serum protein electrophoresis with immunofixation and testing for serum free light chains were performed. Exertional abdominal bloating and dyspnea abated after treatment with furosemide, and spironolactone was started.

Six days after the initial visit in the cardiovascular performance program clinic, results of the serum protein electrophoresis and serum free light-chain assay became available. The serum IgG level was 715 mg per deciliter (reference range, 700 to 1600), the IgA level 29 mg per deciliter (reference range, 66 to 436), and the IgM level 13 mg per deciliter (reference range, 43 to 279). Monoclonal kappa light chain protein was detected on serum immunofixation. The free lambda light-chain level was 3.1 mg per liter (reference range, 5.7 to 26.3), and the free kappa light-chain level was 3653.9 mg per liter (reference range, 3.3 to 19.4), with a kappa:lambda ratio of 1178.68 (reference range, 0.30 to 1.70). The patient was referred to the cancer center of this hospital for a bone marrow biopsy and additional disease management.

CLINICAL DIAGNOSIS

Hypertrophic cardiomyopathy mimic, most likely cardiac amyloidosis.

DR. CLYDE W. YANCY'S DIAGNOSIS

Restrictive cardiomyopathy due to an infiltrative process consistent with amyloidosis.

PATHOLOGICAL DISCUSSION

Dr. Bailey M. Hutchison: Microscopic examination of a core biopsy specimen of bone marrow, stained with hematoxylin and eosin, and a bone marrow aspirate sample, stained with Giemsa, revealed slightly hypercellular marrow for the patient's age (Fig. 2A). Atypical plasma cells with hyperchromatic nuclei were scattered singly and in small clusters throughout the marrow, comprising approximately 40% of the cellularity (as confirmed by means of CD138 and MUM1 immunostaining) (Fig. 2B). In situ hybridization for kappa and lambda light chains showed monotypic kappa expression in the plasma cells. No evidence of amyloid deposition was seen on Congo red staining of the core biopsy specimen.

Three days after the bone marrow biopsy was performed, a fat-pad biopsy specimen was obtained for microscopic examination and immunofluorescence staining, a technique shown to have high sensitivity for the detection of certain types of amyloid.[7] The sections of the specimen stained with hematoxylin and eosin (Fig. 2C) revealed eccentric thickening of focal vessel walls by a pink, waxy substance consistent with amyloid. On Congo red staining, the waxy substance was salmon-pink under standard light microscopy and showed apple-green birefringence under polarized light, findings characteristic of amyloid (Fig. 2D and 2E). Immunofluorescent staining of the fat-pad specimen (Fig. 2F) was positive for kappa light chains, a finding consistent with the light-chain expression of the clonal plasma cells found in the bone marrow. Staining for lambda light chains, transthyretin, serum amyloid A, β_2 microglobulin, apolipoprotein A1, fibrinogen, and IgG, IgA, and IgM heavy chains was negative.

Together, the findings in the bone marrow and fat-pad biopsy specimens were diagnostic of systemic immunoglobulin light-chain (AL) amyloidosis (the abnormal deposition of immunoglobulin light chain secondary to a plasma cell dyscrasia). Fluorescence in situ hybridization was performed on the bone marrow specimen, which revealed the chromosomal translocation t(11;14) in the clonal plasma cells. This translocation results in a cyclin D1:IgH fusion product, a common finding in patients with AL amyloidosis.[8]

PATHOLOGICAL DIAGNOSIS

AL amyloidosis.

ADDITIONAL CARDIAC TESTING

Dr. Rodney H. Falk: A transthoracic echocardiogram obtained 3 weeks after diagnosis of AL amyloidosis showed classic features of amyloid cardiomyopathy; some of these findings had been present on the patient's previous imaging study, but the new study showed evidence of progressive disease (Figs. 3A, 3B, 3C, and 2E). The left and right ventricular walls were thickened, and the left ventricular ejection fraction remained normal (see Videos 1 and 2, available with the full text of this article at NEJM.org). However, speckle-tracking echocardiography with Doppler revealed severe impairment of longitudinal systolic contraction with a global left ventricular strain of –10.1% (reference value, <–19%). The bull's-eye view with color coding of each of the 17 left ventricular segments showed better contraction at the apex than at the base, which is a typical pattern in patients with cardiac amyloidosis known as "apical sparing," which may lessen or disappear in late disease.

A diminutive A wave was observed on transmitral Doppler flow (Fig. 3E); this may occur when the left ventricular filling pressure is high (restrictive pattern), but it is also often seen in patients with amyloidosis due to infiltration of the atria, a condition that leads to atrial contractile dysfunction. On echocardiography, the measurement of left atrial strain (defined as the percentage shortening and lengthening of the atrial wall throughout the cardiac cycle) showed not only severe impairment of left atrial contraction but also impaired atrial filling, most likely a result of a marked increase in stiffness due to amyloid infiltration of the atrial myocardium (see Videos 3 and 4). This stiff atrium syndrome results in elevated left atrial pressure and worsens the congestion associated with ventricular diastolic dysfunction. In this patient, mitral valve thickening due to valvular tissue infiltration (resulting in moderate mitral regurgitation) was present, as was additional evidence of left ventricular diastolic impairment and a dilated inferior vena cava.

Videos showing echocardiograms are available at NEJM.org

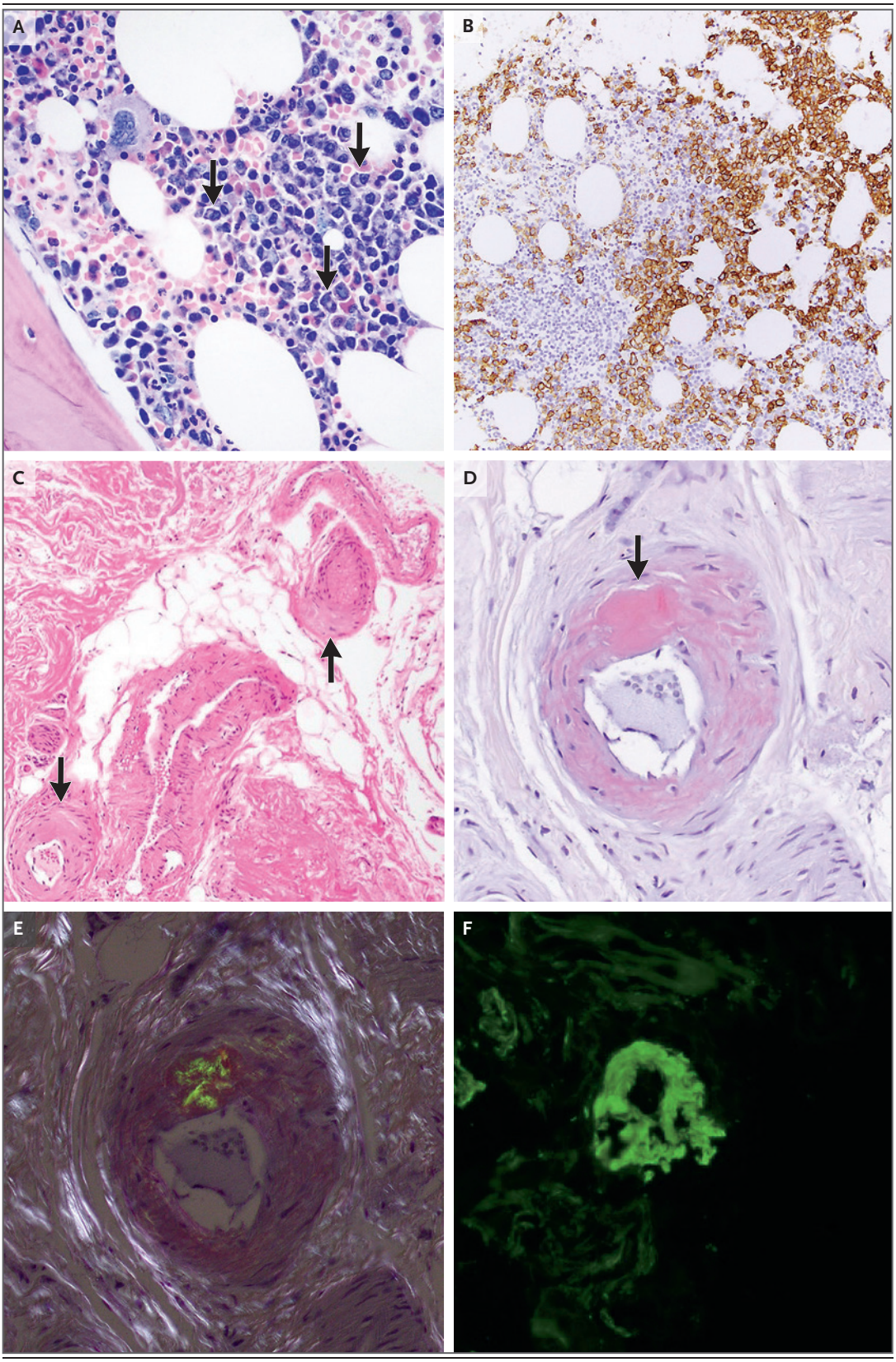

Figure 2 (facing page). Bone Marrow and Fat-Pad Biopsy Specimens.

Giemsa staining of a core biopsy specimen of bone marrow (Panel A) shows a population of atypical plasma cells (representative plasma cells denoted by arrows) infiltrating the marrow as single cells and in small clusters. Immunostaining for CD138 (Panel B) shows that plasma cells account for approximately 40% of the marrow cellularity. Hematoxylin and eosin staining of a section of the fat-pad biopsy specimen (Panel C) reveals eccentric thickening of vessel walls by a waxy substance (arrows). On Congo red staining, the substance is salmon-pink under standard light microscopy (Panel D, arrow) and shows apple-green birefringence under polarized light (Panel E), findings consistent with amyloid. Immunofluorescent staining of the fat-pad biopsy specimen was positive for kappa light chain (Panel F) and negative for all other tested antigens, a finding that, when considered together with the bone marrow biopsy findings, is diagnostic of AL amyloidosis.

Dr. Ghoshhajra: The patient underwent repeat cardiac MRI (Fig. 4A), which revealed biatrial enlargement and continued concentric left ventricular wall thickening. In the interim, after the initial scan was performed, scanner-specific reference myocardial normal values had been established, and standard longitudinal relaxation time (T1) and transverse relaxation time (T2) mapping had been implemented in all cardiac MRI protocols; myocardial T1 relaxation values were markedly elevated at 1182 msec (reference range, 938 to 1094) (Fig. 4B). Qualitative findings consistent with cardiac amyloidosis included biventricular thickening, biventricular and biatrial abnormal late gadolinium enhancement, and gadolinium kinetics consistent with a marked expansion of extracellular space uptake. The initial cardiac MRI performed 2 years earlier was compared with the most recent imaging studies, highlighting a progression of disease and overall findings that were most consistent with a diagnosis of AL amyloidosis.

DISCUSSION OF MANAGEMENT

Dr. Andrew J. Yee: Treatment of AL amyloidosis borrows from regimens used for the treatment of multiple myeloma. With effective treatment and hematologic responses, there can be improvement in function of the affected organs and a better prognosis.[9]

The proteasome inhibitor bortezomib is commonly used to treat AL amyloidosis, especially in combination with cyclophosphamide and dexamethasone (CyBorD).[10] In addition, the anti-CD38 monoclonal antibody daratumumab is now used with the CyBorD regimen on the basis of the results of the ANDROMEDA trial,[11] and this treatment regimen was selected for this patient. This phase 3 trial evaluated the use of daratumumab with CyBorD (daratumumab group) as compared with CyBorD alone (control group) in patients with a new diagnosis of AL amyloidosis. Of note, the trial excluded patients with severe cardiac involvement (defined as an N-terminal pro–B-type natriuretic peptide level of >8500 ng per liter, a systolic blood pressure of <90 mm Hg, or a New York Heart Association classification of stage IIIB or IV at screening). The trial showed that the addition of daratumumab was associated with a significantly higher percentage of patients with a hematologic complete response (53.3% in the daratumumab group vs. 18.1% in the control group; relative risk ratio, 2.9; 95% confidence interval [CI], 2.1 to 4.1; P<0.001). In addition, survival free from major organ deterioration or hematologic progression also favored the daratumumab group, with a hazard ratio of 0.58 (95% CI, 0.36 to 0.93). Treatments that target the amyloid deposits themselves, such as the monoclonal antibodies birtamimab and anselamimab, are under investigation.[12,13]

FOLLOW-UP

Dr. Falk: Patients with cardiac amyloidosis and atrial contractile dysfunction are at increased risk for left atrial thrombus formation, and treatment with apixaban was started even though the patient was initially in sinus rhythm. Atrial myocardial infiltration by amyloid is associated with subsequent development of atrial fibrillation, which later occurred in this patient. The absence of atrial contraction during sinus rhythm might be expected to cause minimal symptomatic deterioration with the onset of atrial fibrillation (since there is no atrial kick to lose); however, when atrial fibrillation develops in patients with amyloidosis, deterioration typically occurs, even if the ventricular rate is not excessively high, which is most likely the result of an irregular rhythm on cardiac hemodynamics.[14] This patient's cardiac symptoms worsened after the onset of atrial fibrillation, and treatment with amiodarone was initiated as a precursor to

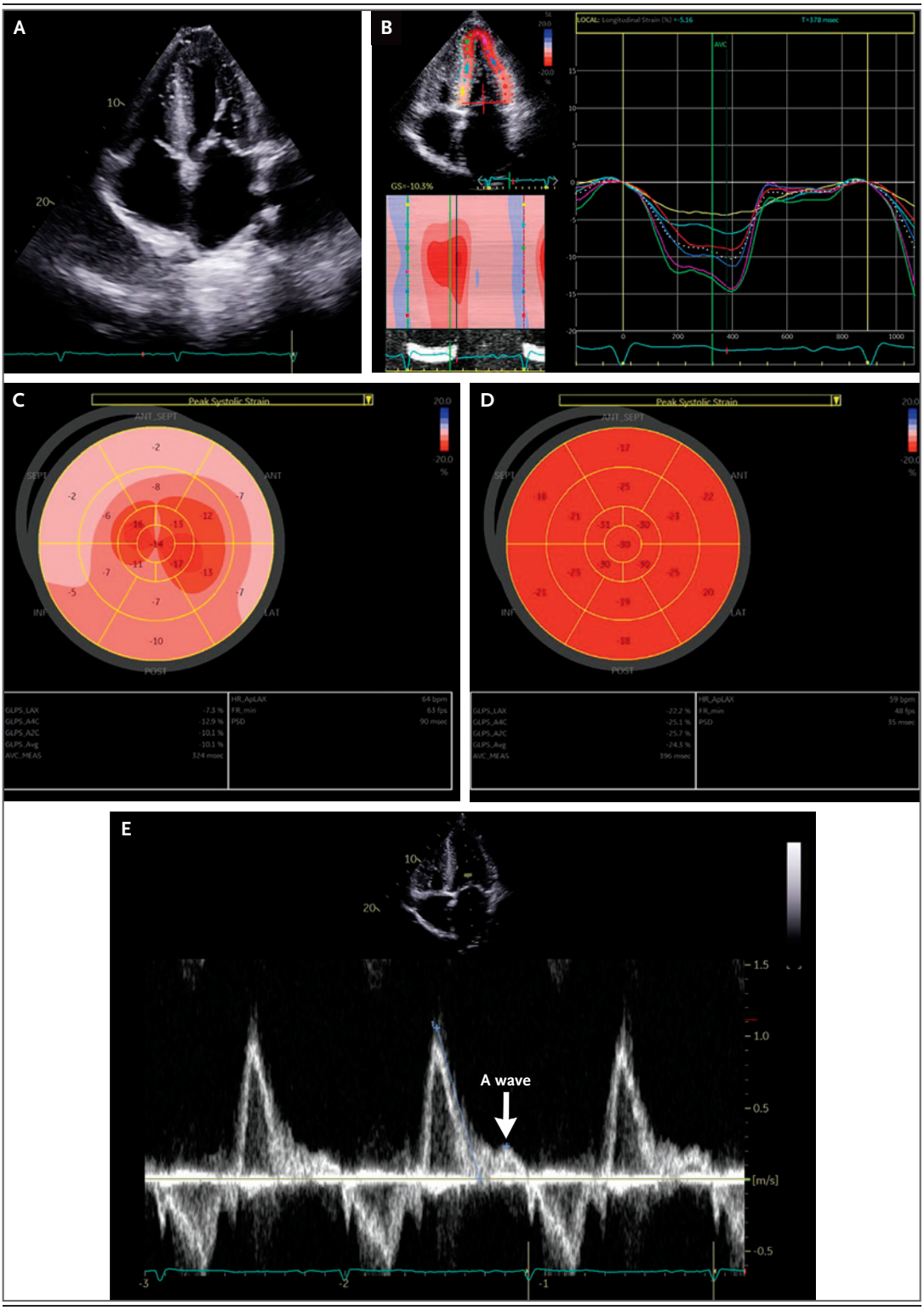

electrical cardioversion. The alternative of catheter-based pulmonary venous isolation for terminating atrial fibrillation, although more effective in the context of many other diseases, has poor efficacy in the infiltrated atrium in patients with amyloidosis.[15] Patients with cardiac involvement

Figure 3 (facing page). Transthoracic Echocardiogram and Strain Imaging.

A transthoracic echocardiogram was obtained 3 weeks after diagnosis of AL amyloidosis. An apical four-chamber view of the left ventricle (Panel A) and a speckle-tracking echocardiogram with Doppler (Panel B) show color-coded longitudinal left ventricular contraction, with red indicating greater relative contraction, seen predominantly in the apical segments in an apical-sparing pattern, typical of amyloidosis. Bull's-eye views of the global longitudinal left ventricular strain in this patient (Panel C) and in a healthy patient (Panel D) show overall severe reduction in strain in this patient with amyloid cardiomyopathy, with relative sparing at the left ventricular apex, a classic finding in amyloid cardiomyopathy. A transmitral pulsed Doppler study (Panel E) shows a very small A wave with normal deceleration time, a finding suggestive of left atrial contractile dysfunction.

associated with AL amyloidosis have a poor prognosis and often die from progressive heart failure or sudden cardiac death; prophylactic implantable defibrillators are rarely effective.[16]

Dr. Guseh: The patient continued to take diuretic agents and was continuing submaximal aerobic and weight exercise. Unfortunately, between the third and fourth chemotherapy cycles, the patient had a cardiac arrest at home during the night and could not be resuscitated.

FINAL DIAGNOSIS

AL amyloidosis.

CASE RECORDS EDITORS' NOTE — LESSONS LEARNED

1. The presence of Kussmaul's sign was a key examination finding that prompted consideration of restrictive cardiomyopathies.

2. This patient was originally given a diagnosis of nonobstructive hypertrophic cardiomyopathy on the basis of a previous echocardiogram that showed concentric left ventricular wall thickening of 17 mm and preserved ejection fraction. This represents a common error, namely mischaracterization of left ventricular wall thickening (a descriptive diagnosis) as left ventricular hypertrophy (a pathological diagnosis). Although most cases of increased left ventricular wall thickness do represent true hypertrophy, the differential diagnosis must include an infiltrative process, of which the most common is amyloidosis.

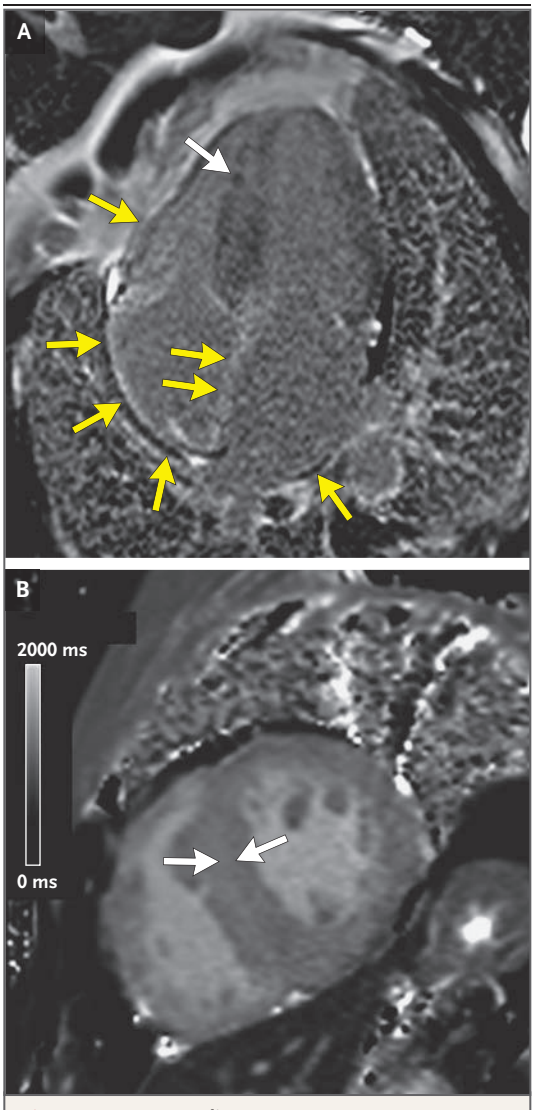

Figure 4. Repeat Cardiac MRI.

Selected images from repeat cardiac MRI reveal increased nonischemic, nonterritorial abnormal late gadolinium enhancement (Panel A), which now affects the mid-interventricular septum (white arrow) as well as the right ventricle and both atria (yellow arrows). Both atria are also enlarged. In addition to persistent wall thickening, myocardial T1 relaxation values are markedly elevated (Panel B) at 1182 msec (reference range, 938 to 1094), with increased signal evident in the mid-ventricular septum (arrows).

3. Amyloidosis is associated with concentric left ventricular wall thickening (as this patient had), and right ventricular wall thickening may be present. In contrast, hypertrophic cardiomyopathy is usually associated with asymmetric septal hypertrophy (although other distributions and

variants are possible) and right ventricular wall thickening is rare.

4. Hoarseness is a feature of amyloidosis that is caused by vocal cord infiltration. It is a clue to the type of amyloid, as it is almost exclusively limited to AL (and not transthyretin) amyloidosis. Of course, marked left atrial enlargement can also affect the recurrent laryngeal nerve and lead to hoarseness.

5. Although serum protein electrophoresis is a part of the laboratory workup for AL amyloidosis, it may be negative in up to 50% of patients. Thus, if only serum protein electrophoresis, or "serum protein electrophoresis with reflex immunofixation," is ordered, an abnormal result on serum immunofixation (seen in approximately 85% of patients with AL amyloidosis) will be missed. This is a common error, since free light chains are often not obtained unless immunofixation (serum or urine) has abnormal results.

This case was presented at Cardiology Grand Rounds.

Disclosure forms provided by the authors are available with the full text of this article at NEJM.org.

REFERENCES

1. Dudzinski DM, Pellikka PA. Systemic light chain amyloidosis. N Engl J Med 2024;391:1165.

2. Pellikka PA, Dudzinski DM, Lubitz SA, Tsang TSM, Tower-Rader A, Karaa A. Case Records of the Massachusetts General Hospital (Case 10-2022). N Engl J Med 2022;386:1266-76.

3. Muchtar E, Blauwet LA, Gertz MA. Restrictive cardiomyopathy: genetics, pathogenesis, clinical manifestations, diagnosis, and therapy. Circ Res 2017;121:819-37.

4. Newton-Cheh C, Lin AE, Baggish AL, Wang H. Case Records of the Massachusetts General Hospital (Case 11-2011). N Engl J Med 2011;364:1450-60.

5. Raja MHR, Javed MA, Zubairi ABS. Sarcoidosis presenting as vocal cord palsy: an unusual presentation and literature review. Respirol Case Rep 2021;9(2):e00705.

6. Sueyoshi T, Ueda M, Jono H, et al. Wild-type transthyretin-derived amyloidosis in various ligaments and tendons. Hum Pathol 2011;42:1259-64.

7. Garcia Y, Collins AB, Stone JR. Abdominal fat pad excisional biopsy for the diagnosis and typing of systemic amyloidosis. Hum Pathol 2018;72:71-9.

8. Bryce AH, Ketterling RP, Gertz MA, et al. Translocation t(11;14) and survival of patients with light chain (AL) amyloidosis. Haematologica 2009;94:380-6.

9. Ravichandran S, Lachmann HJ, Wechalekar AD. Epidemiologic and survival trends in amyloidosis, 1987–2019. N Engl J Med 2020;382:1567-8.

10. Mikhael JR, Schuster SR, Jimenez-Zepeda VH, et al. Cyclophosphamide-bortezomib-dexamethasone (CyBorD) produces rapid and complete hematologic response in patients with AL amyloidosis. Blood 2012;119:4391-4.

11. Kastritis E, Palladini G, Minnema MC, et al. Daratumumab-based treatment for immunoglobulin light-chain amyloidosis. N Engl J Med 2021;385:46-58.

12. Gertz MA, Sanchorawala V, Wechalekar AD, et al. Birtamimab in patients with Mayo stage IV AL amyloidosis: rationale for confirmatory affirm-AL phase 3 study. Blood 2022;40(16)Suppl:TPS8076. abstract.

13. Wechalekar AD, Silowsky J, Daniel E, et al. Cardiac Amyloid Reaching for Extended Survival (CARES): study design of two placebo-controlled, double-blind, randomized, international phase 3 trials assessing Cael-101 in patients with Mayo stage Iiia or stage IIIb AL amyloidosis. Blood 2021;138:Suppl 1:1673 (https://ashpublications.org/blood/article/138/Supplement%201/1673/480200/Cardiac-Amyloid-Reaching-for-Extended-Survival).

14. Stojadinović P, Deshraju A, Wichterle D, et al. The hemodynamic effect of simulated atrial fibrillation on left ventricular function. J Cardiovasc Electrophysiol 2022;33:2569-77.

15. Barbhaiya CR, Kumar S, Baldinger SH, et al. Electrophysiologic assessment of conduction abnormalities and atrial arrhythmias associated with amyloid cardiomyopathy. Heart Rhythm 2016;13:383-90.

16. Falk RH. Cardiac amyloidosis: a treatable disease, often overlooked. Circulation 2011;124:1079-85.